ISSN 1990-519X, Cell and Tissue Biology, 2018, Vol. 12, No. 2, pp. 127–134. © Pleiades Publishing, Ltd., 2018.
Original Russian Text © S.N. Pleskova, E.E. Gornostaeva, R.N. Kryukov, A.V. Boryakov, S.Yu. Zubkov, 2017, published in Tsitologiya, 2017, Vol. 59, No. 12, pp. 874–880.

Changes in the Architectonics and Morphometric Characteristics of Erythocytes under the Influence of Magnetite Nanoparticles

S. N. Pleskova[a], *, E. E. Gornostaeva[b], R. N. Kryukov[a], A. V. Boryakov[b], and S. Yu. Zubkov[a]

[a] *Research and Education Center Physics for Solid State Nanostructures, Nizhny Novgorod State University, Nizhny Novgorod, 603950 Russia*

[b] *New Materials and Resource-Saving Technologies Center of Collective Use of the Scientific Research Institute of Chemistry of Nizhny Novgorod State University, Nizhny Novgorod, 603950 Russia*

**e-mail: pleskova@mail.ru*

Received July 27, 2017

Abstract—A new high-precision technique for calculating the ratio of the erythrocyte area/volume using atomic-force microscopy has been developed. The method was tested on erythrocytes of healthy donors. Scanning electron microscopy, atomic-force microscopy, and X-ray microanalysis revealed that magnetite nanoparticles can interact with erythrocyte membranes in vitro. This interaction resulted in the development of a pathology of erythrocytes typical for poikilocytosis and anisocytosis. When the magnetite was incubated with erythrocytes in a serum-free medium, nanoparticles aggregated.

Keywords: erythrocytes, area/volume ratio, magnetite nanoparticles, archytectonics, atomic-force microscopy, scanning electron microscopy, X-ray microanalysis

DOI: 10.1134/S1990519X18020086

INTRODUCTION

Erythrocytes can be considered as a kind of "cellular dosimeter" of the action of endo- and exogenous factors and as a unique model for assessing the condition of an organism (Novitsky et al., 2003). The methodological ease of the use of erythrocytes is due to the simple structure of their membranes, which, nevertheless, retain the functional properties and principle of organization of most cellular types; they exhibit a variety of membrane pathology and can be obtained for research relatively easily (Leonova, 1987). At the same time, the significance of the analysis of the main morphological parameters of erythrocytes, e.g., identification of architectonics characteristics and the analysis of the ratio of area to volume, is due to the essential role played by erythrocytes in maintaining homeostasis. Red blood cells, in addition to a specific gas-transport function, take part in the regulation of the acid–alkaline and water–electrolyte balance, in the microrheological status of blood, and in immune reactions. They also bind and transfer amino acids, lipids, viruses, and drugs (Novitsky et al., 2003). Thus, it is important to find new, highly accurate methods for assessing the structural and morphological features of red blood cells.

Abbreviations: AFM—atomic-force microscopy, MNPs—magnetite nanoparticles, SEM—scanning electron microscopy, PBS—phosphate buffer saline.

Magnetite nanoparticles (MNPs) are used in medicine, primarily due to their ability to be controlled remotely under the influence of an external magnetic field. The main areas of use of MNPs are increasing the contrast and sensitivity of magnetic resonance imaging, directed drug delivery, hyperthermia in the treatment of malignant neoplasms, and diagnostics in vitro (Pankhurst et al., 2003; Bulte and Kraitchman, 2004; Grancharov et al., 2005; Neamtu and Verga, 2011; Guo et al., 2013). To use MNPs in vivo, they must meet the following requirements: they must (1) form a stable colloidal system in aqueous solutions; (2) be resistant to changes in salt concentrations, pH, and temperature over sufficiently wide ranges; and (3) have equal dimensions and not aggregate (Pershina et al., 2008). First of all, though, it is necessary that MNPs not cause significant morphofunctional changes in blood cells. Yakusheva et al. (2013) showed that intramuscular injection of iron nanoparticles (2 mg per kg of animal weight) to rats leads to a significant increase in the number of erythrocytes and the concentration and average content of hemoglobin, on both the first and seventh days of study (Yakusheva et al., 2013). After a single intragastric administration of γ-Fe_2O_3 maghemite to rats (100 mg/mL), the number of erythrocytes decreased with a sharp increase in the hemoglobin concentration; in addition, the volume, height, and surface area of the cell decreased with an unchanged erythrocyte diameter (Skorkina

et al., 2010). This contradicts the data of other authors, who showed that MNPs coated with citric acid did not cause hemolysis, aggregation, or changes in the morphology of erythrocytes in vitro (Nasiri et al., 2016).

Thus, the first aim of this study was to develop a technique for estimating the area/volume ratio using atomic-force microscopy (AFM). Unlike electron microscopy, AFM allows one to measure all the main parameters of cells (diameter, height, volume, and surface area) with high accuracy and to conduct dynamic studies in a physiological environment on cells with pronounced adhesion properties without using fixation (Pleskova, 2011). The second aim of the study was to determine the main morphological parameters of erythrocytes after incubation with MNPs by AFM, to elucidate the changes in the cells' architecture by scanning electron microscopy (SEM), and to evaluate the possibilities of MNPs interaction with erythrocyte membranes by X-ray microanalysis.

MATERIAL AND METHODS

Cell separation. Venous blood of healthy donors of both genders from 20 to 40 years of age was examined. Blood sampling was performed in the morning after the donors had signed an informed-consent form. After a centrifugation (200*g*, 3 min) of heparinized blood (50 U/ml) and decanting the plasma and the leukocyte-platelet layer, the erythrocytes were washed five times with PBS containing 0.137 M NaCl and 0.0027 M KCl, pH 7.35. Twenty microliters of red blood cells were removed and diluted 50-fold, and so the initial cell concentration was 1×10^6 cells/mL (according to a Goryaev's chamber). Erythrocytes were incubated with MNPs in a ratio of 9 : 1 (experiment) or with an equivalent amount of PBS (control) for 60 min at 37°C (Pleskova et al., 2013).

Characteristics of nanoparticles. MNPs ($FeO \cdot Fe_2O_3$) were kindly provided by D.A. Gorin (Department of Semiconductor Physics, Saratov State University). Particles were obtained by chemical precipitation from a solution of iron salts (Fe (II) and Fe (III)) and stabilized with citric acid (Herman et al., 2013a). The hydrodynamic diameter and the ζ-potential of the MNPs were measured on a ZetasizerNano device (Malvern Instruments Ltd., United Kingdom); the indices were 20 ± 4 nm and -13.09 mV, respectively. Prior to the experiments. the MNPs were shaken in a Vortex (ELMI Ltd., Latvia) for 10 min, dispersed in an ultrasonic bath (RELTEK, Moscow) for 15 min to achieve homogeneity, and then used for incubation with erythrocytes in final concentrations that did not affect the viability of neutrophils—0.0018 and 0.18 mg/mL (Herman et al., 2013b).

AFM. Erythrocytes were transferred to the surface of glass microscope slides and fixed with glutaraldehyde (2.5%, 20 min, 24°C), washed three times in FBS, and scanned in the semicontact mode on air using an Ntegra Spectra device (NT-MDT, Russia). To process the scan results, the software package Gwyddion (Faculty of Nanometrology of the Czech Metrological Institute, Czech Republic) was used. DNP probes (Bruker, United States) with a tip radius of 20 nm, a front angle of 15°, a resonant frequency of about 65 kHz, and a spring constant of 0.35 N/m were used. The main morphological parameters of erythrocytes—the diameter, height in the area of tor, height in the zone of the pellor (if one was formed), surface area, and volume—were evaluated in the Gwyddion package.

SEM and X-ray microanalysis. The cells were prepared as for AFM but aluminum or gold (Au/GaAs) was used as the surface. The use of two materials with different atomic numbers is due to the need to obtain scans of different contrast levels. The studies were carried out on a JSM-IT300LV electron microscope (JEOL, Japan) in the high-vacuum mode with an accelerating voltage of 5 kV and 20 kV, with an electron-beam diameter reaching 5 nm. For the X-ray microanalysis, an X-MaxN 20 Silicon Drift Detector (Oxford Instruments, United Kingdom) was used, with the spatial resolution being ~0.25 μm. The X-ray microanalysis mode was used for constructing maps of the distribution of elements (raster scanning 256 × 256 or 512 × 512 points) over the surface and determining the composition at certain points. The accumulation time of the entire map was about 1 h, and each individual point of the scan experienced accumulation of its own spectrum. The beam current did not exceed 0.5 nA so as to minimize the effect on the cells.

Statistical analysis. The boundaries of the normal distribution of quantitative sampling parameters were determined using the Shapiro–Wilk test. In the case of a normal distribution, Student's test for independent samples (parametric statistics) was used to compare the variances of means of control and experiment. In the case of an abnormal distribution, a two-sample Wilcoxon test (nonparametric statistics) was used. The differences between the two samples were considered statistically significant at $p < 0.05$. For statistical analysis, we used the Origin Pro 8 software (OriginLab Corp., United States).

RESULTS AND DISCUSSION

Normocytes are characterized by a high ratio of surface area to volume, which ensures maximum closeness of hemoglobin to the surface and, thus, a maximum gas-exchange rate (Borovskaya et al., 2010). The area/volume ratio decreases with the transformation of erythrocytes into any pathological form. We propose a method for the accurate quantification of the main cell parameters based on measurements of erythrocytes by AFM, in which the microscope scans of the cell surface, providing an array of data that is transformed into a real 3D image. The image-process-

ing program then allows one to measure the surface area of the erythrocyte, the cell's projected area, the volume of the erythrocyte (Fig. 1), and its height and diameter (Fig. 2) with nanometer accuracy.

It is known (O'Reilly et al., 2001) that the procedure for immobilizing erythrocytes on a substrate in preparation for AFM does not lead to quantitative artifacts, since the average volume of immobilized cells correlates exactly with the parameters of the average cell volume used in modern hematological practice.

We suggest evaluating the ratio of the erythrocyte area/volume according to the following formula:

$$\frac{S}{V} = \frac{\text{erythrocyte surface area} + \text{erythrocyte projected area}}{\text{erythrocyte volume}}, \quad (1)$$

where S is erythrocyte surface area and V is erythrocyte volume.

Two factors are fundamental for correct estimation of the ratio and other parameters (height, diameter) of the cell: (1) accurate calibration of the AFM before scanning and (2) use of the correct fixation method. According to the data obtained by the combination of Raman microspectroscopy and AFM, two fixation methods provide the maximum structural integrity of red blood cells and the preservation of hemoglobin: fixation with glutaraldehyde and with a mixture of formaldehyde (3%) and glutaraldehyde (0.1%). In the latter case, cell autofluorescence is minimal (Asghari-Khiavi et al., 2010). We used fixation with glutaraldehyde (2.5%), which provides the maximum preservation of erythrocyte's architectonics. Approbation of the method of quantitative evaluation of the main parameters on the erythrocytes of healthy donors showed that the cell height in the area of tor was 1.70 ± 0.54 μm; in the zone of the pellor, 0.22 ± 0.16 μm; the cell diameter was 8.56 ± 0.95 μm; the total cell surface area was 105.59 ± 12.82 μm^2; the volume of cells was 61.55 ± 9.13 μm^3; and the area/volume ratio was 2.07 ± 0.34 (Fig. 2, Table 1).

In the control (incubation in PBS without MNPs, 60 min, 37°C), the predominant form of erythrocytes was normocytes. Both SEM and AFM showed distinctive classical form of biconcave disks (Fig. 2, 3). X-ray microanalysis showed the presence of organic elements only (carbon and oxygen) (Fig. 3b). However, even such a short incubation in a glucose-free environment led to a slight transformation of cells: the amount of normocytes was 88.9% of the total number of erythrocytes, the amount of echinocytes was 2.3%, and the amount of cells of other

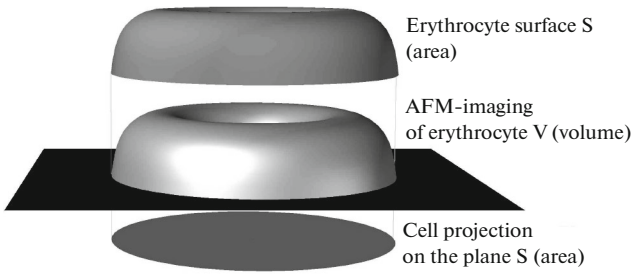

Fig. 1. Scheme of measuring the S/V ratio of erythrocyte. The surface area of the erythrocyte (the upper part of the cell) and the lower part of the cell associated with the substrate (the projection of the cell on the plane) had been summed and divided by the volume of the erythrocyte.

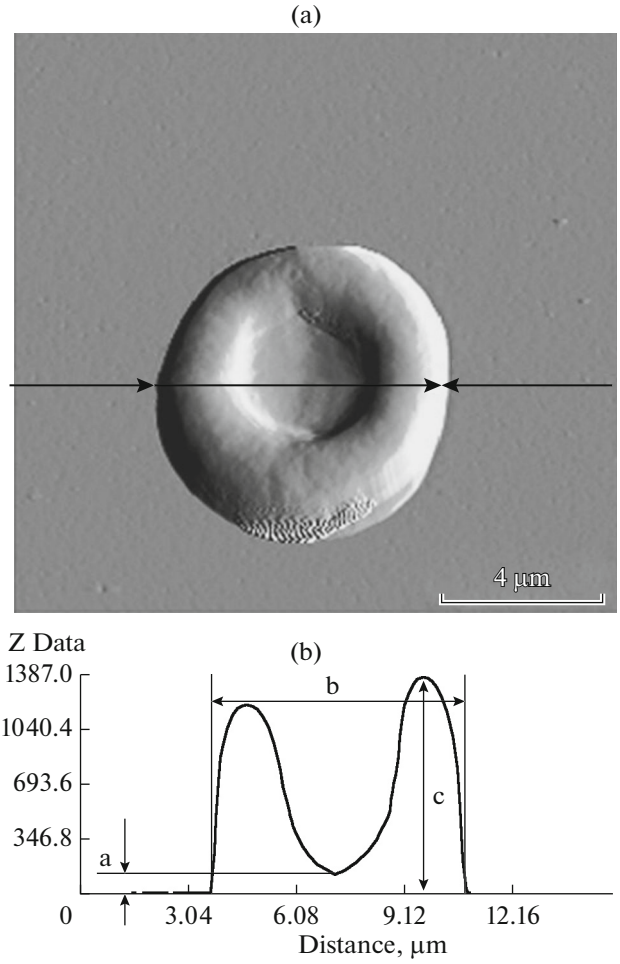

Fig. 2. Morphometric characteristics of erythrocyte (cell obtained by AFM). (*a*) Architectonics of a typical normocyte, (b) the lateral profile of the cell shows the principle of measuring the main parameters of the erythrocyte (a) height in the pellor, (b) erythrocyte diameter, and (c) height in the area of tor.

Table 1. The main morphological parameters of erythrocytes in the control and after interaction with MNPs (37°C, 60 min)

MNPs concentration, mg/mL	Erythrocyte diameter, μm	Maximal height (in the area of tor), μm	Minimal height (in the area of pellor), μm	Surface area of erythrocyte, μm^2	Erythrocyte volume, μm^3	Area/surface ratio
Control	8.56 ± 0.95 (n = 82)	1.70 ± 0.54 (n = 76)	0.22 ± 0.16 (n = 53)	105.59 ± 12.82 (n = 41)	61.55 ± 9.13 (n = 34)	2.07 ± 0.34 (n = 47)
0.0018	7.58 ± 0.85* (n = 122)	2.11 ± 0.50* (n = 130)	0.62 ± 0.32* (n = 56)	100.25 ± 18.92* (n = 65)	53.65 ± 10.22* (n = 68)	2.05 ± 0.20 (n = 42)
0.18	7.44 ± 0.99* (n = 71)	1.90 ± 0.52* (n = 76)	0.80 ± 0.44* (n = 41)	99.77 ± 11.22 (n = 39)	52.38 ± 8.36* (n = 60)	1.90 ± 0.25* (n = 43)

n is number of experiments.

* Differences with the control are statistically significant ($p < 0.05$).

forms was 8.8% (according to the results of the analysis of the architectonics of 100 cells by AFM). Analysis of erythrocytes using the SEM method also revealed an absolute prevalence of normocytes. In some cases, an unusual "triangular" form of the central zone of pellor was found in normocytes. The surface of all cells was smooth, and the membrane was clearly contoured.

In case of incubation of erythrocytes with MNPs, the latter had aggregated. This was manifested in an increase in the hydrodynamic diameter from 20 ± 4 to 37 ± 4 nm ($p < 0.05$). The phenomenon of increasing the hydrodynamic diameter due to interaction with serum proteins and formation of the so-called "protein crown" around the nanoparticles (from albumins, immunoglobulins, complement system proteins, apolipoprotein, transferrin, hemoglobin) is an established fact (Duran et al., 2015). However, in our study, incubation of MNPs with serum resulted in only a slight increase in diameter to 28 ± 2 nm, whereas a change in MNPs size after incubation with erythrocytes led to an increase in their hydrodynamic diameter. Hemoglobin released from erythrocytes due to damage to the cell membranes is probably responsible for the formation of the "protein crown" in this case. Therefore, to isolate MNPs from blood cells and maintain the original degree of their dispersion, it is necessary to use inert coatings or to enclose them in liposomes.

Incubation of erythrocytes with MNPs led to a significant change in the architectonics of cells and damaged the erythrocyte membranes. Transformation of erythrocytes was assessed according to the atlases of Novitsky et al. (2003) and Kozinets et al. (2004).

The following transformed erythrocyte forms were detected by SEM after incubation with MNPs at a final concentration of 0.18 mg/mL (37°C, 60 min): dacrocytes, erythrocytes in the form of a teardrop (Fig. 4a); spherocytes, erythrocytes in the form of a sphere (Fig. 4b); stomatocytes, dome-shaped cells with a hollow (Fig. 4c); and codocytes, erythrocytes in the form of a bell (Fig. 4d). The microstructure of the erythrocyte membranes also was significantly altered: the cell surface was uneven, "spongy," and, in some parts of the cell, significantly deformed. Obviously, large MNPs aggregates directly interact with erythro-

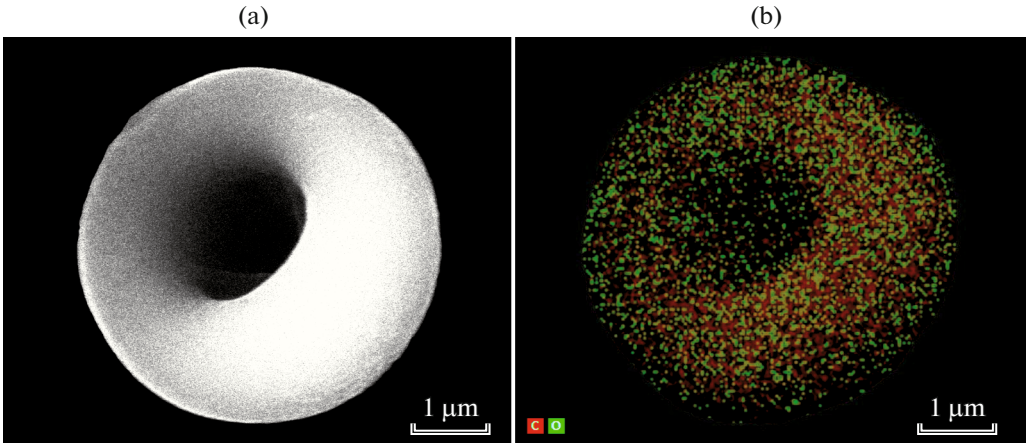

Fig. 3. Structural-morphological characteristics of erythrocyte. (a) Architectonics of a typical normocyte (cell obtained by SEM), (b) map of carbon (red) and oxygen (green) distribution in a cell, (obtained by X-ray microanalysis).

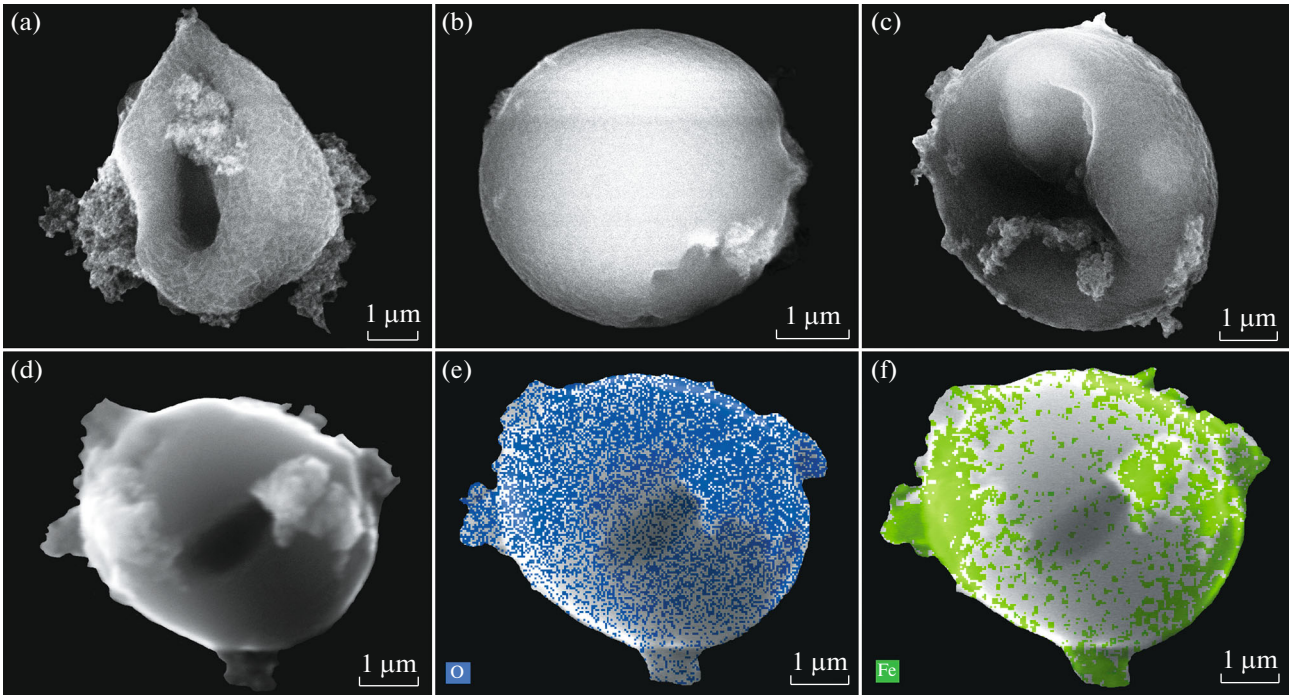

Fig. 4. Images of erythrocytes transformed under the influence of MNPs obtained by SEM and X-ray microanalysis. (a) Architectonics of dacryocyte, (b) architectonics of spherocyte, (c) architectonics of codocyte, (d) architectonics of stomatocyte (SEM), (e) map of oxygen distribution (*blue*) in stomatocyte, and (*f*) map of iron distribution (*green*) in stomatocyte (X-ray microanalysis; Kα-lines O and Fe). Colocalization of Fe and O signals in the region of visible aggregates confirms direct binding of MNPs with the stomatocyte membrane.

cyte membranes that are damaged as a result. X-ray microanalysis data also directly indicated the binding of large MNPs aggregates with erythrocytes: there was a colocalization of signals from Fe and O in the region of visible aggregates (Figs. 4d, 4e).

AFM yielded a similar result indicating the transformation of erythrocytes in the process of interaction with MNPs (0.0018 mg/mL, 37°C, 60 min). The following transformed forms of erythrocytes were identified (Fig. 5): (a) spherocytes, (b) stomatocytes, (c) codocytes, and (d) echinocytes.

As in case of SEM, direct binding of MNPs aggregates to erythrocyte membranes was observed (Fig. 5d), resulting in the cell-membrane damage (Fig. 5e). We noted the appearance of "cracks" on the surface of the membrane. The membrane lost its smoothness and structure. One of the possible variants of alteration is the destruction of sialic acid, as it causes a negative charge of membranes and prevents the aggregation of red blood cells. This mechanism was confirmed by visualization of large shapeless aggregates of cells formed by erythrocytes after incubation with MNPs.

A significant shift of the erythrogram toward the transformed forms was also revealed. Incubation with MNPs at a final concentration of 0.0018 mg/mL gave the following erythrogram (%): normocytes, 51.4; spherocytes, 30.6; echinocytes, 10; and other forms, 8 (according to the results of AFM of the architectonics of 100 cells). Incubation with MNPs at a final concentration of 0.18 mg/mL yielded an even greater shift of the erythrogram toward prehemolytic forms, and the overwhelming majority of red blood cells were spherocytes (%). The erythrogram was as follows (%): normocytes, 9; spherocytes, 64; codocytes, 19; and other forms, 8 (according to the results of AFM analysis of the architectonics of 100 cells).

The results of morphometric analysis confirmed that there was a shift of the erythrogram toward spherocytosis, since incubation with MNPs (both concentrations) caused a statistically significant decrease in diameter simultaneously with an increase in cell height ($p < 0.05$, Table 1). In addition, it seemed there was also a shift toward microspherocytosis, as both the area and the volume of erythrocytes significantly decreased. The area/volume ratio decreased with increasing MNPs concentration to 0.18 mg/mL, which indicated the difficulty of the implementation of the basic gas-transport function by transformed erythrocytes.

Thus, the proposed technique for determining the area/volume ratio completely coincides with the results of other morphometric measurements, and with a morphological evaluation of the changes in the architectonics of erythrocytes under the influence of altering factors. The long-term presence in the blood

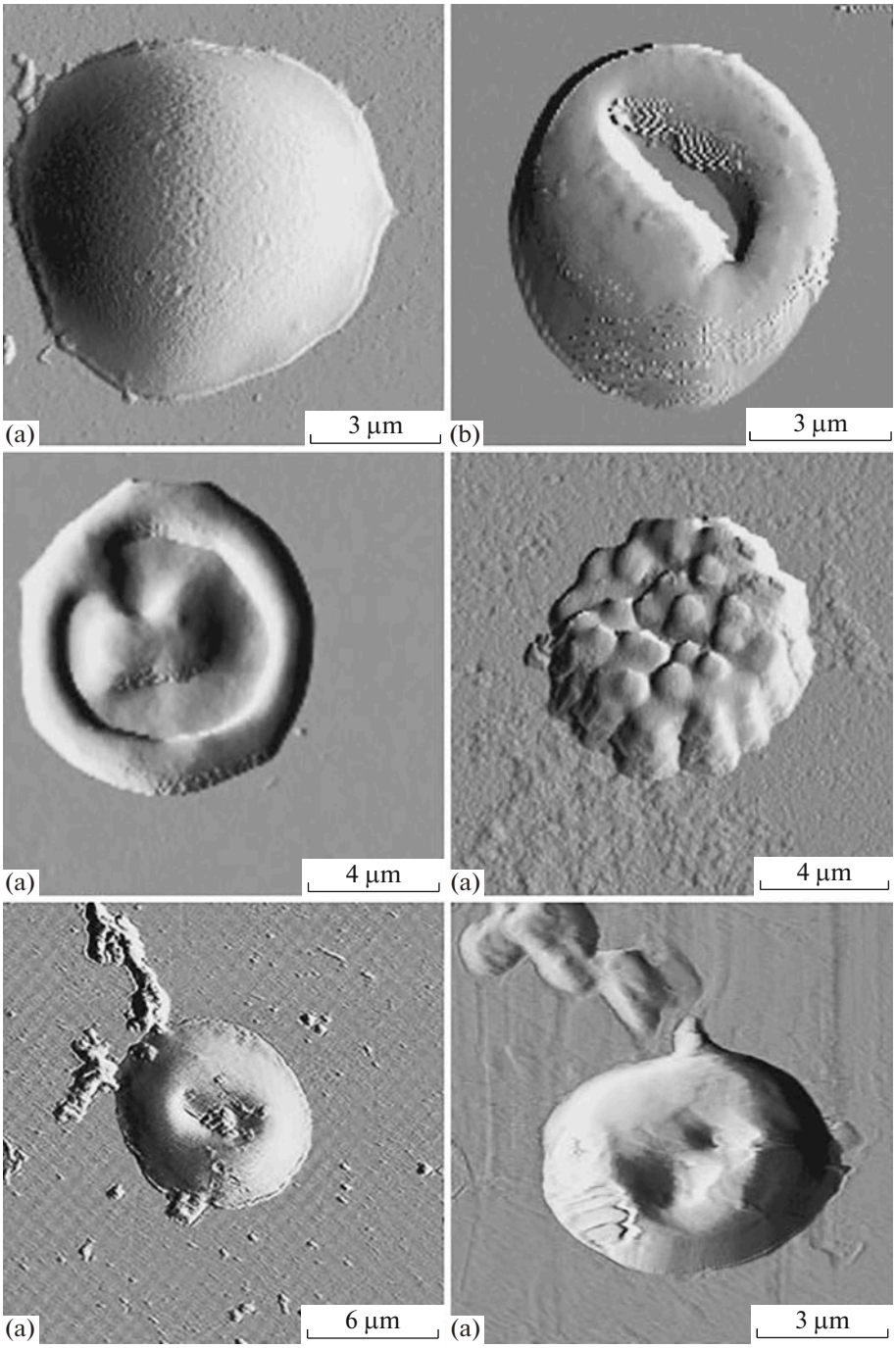

Fig. 5. The effect of MNPs on the structural and morphological characteristics of erythrocytes. The images were obtained by AFM. (a) Architectonics of spherocyte, (b) architectonics of stomatocyte, (c) architectonics of codocyte, (d) architectonics of echinocyte, (e) nanoparticles of $FeO \cdot Fe_2O_3$ are bound with erythrocyte membrane, and (f) damage to codocyte membrane under the influence of $FeO \cdot Fe_2O_3$ nanoparticles.

(for 60 min or more) of MNPs even in concentrations harmless to neutrophils (Herman et al., 2013) leads to a pronounced alteration of erythrocytes. This is manifested in a change in the architectonics, morphometric parameters, and microstructure of cell membranes in the erythrogram shift toward the formation of prehemolytic forms (mainly spherocytes), in direct damage to erythrocyte membranes, and changes in the surface charge of membranes, which resulted in the formation of unformed cell aggregates. To prevent these alterations, it is necessary to isolate MNPs from blood cells, for example, by enclosing them in liposomes (German et al., 2015), which can (1) maintain the degree of dispersion and homogeneity of nanoparti-

cles; (2) prevent direct contact of MNPs with blood-cell membranes and, therefore, their alteration; and (3) change the physicochemical properties of nanomaterials, changing them from hydrophilic to hydrophobic.

The interaction between erythrocytes and MNPs aggregates seems to be nonspecific. Electrostatic binding at the initial stage is impossible because of the negative charge on the erythrocyte membrane and the negative ζ-potential of the MNPs (–13.09 mV). Hydrophilic (hydrophobic) interactions are also excluded, since membranes are hydrophobic, whereas MNPs are hydrophilic. However, since there is considerable aggregation of MNPs, the following sequence of events can be seen: large MNPs aggregates initially electrostatically bind to positively charged tetraalkylammonium groups of lectin and sphingomyelin. When the aggregates of MNPs converge with the membrane, the sialic acids decompose with a significant decrease in the negatively charged carboxyl groups, which leads to the strengthening of the contact of the MNPs aggregates with the erythrocyte membrane and the addition of short-range van der Waals forces (including London dispersion ones) to the interaction. Direct contact of MNPs with phospholipids of cell membranes can lead to both direct destruction of a number of functional groups and indirect activation of the process of lipid peroxidation, as a result of which membrane stiffness begins to increase due to the predominance of saturated fatty acids. A change in the physicochemical properties of membranes leads to difficulties in the correct function of ion channels (direct contact of MNPs with protein of ion channels, which causes denaturation of the latter cannot also be excluded), and, as a result, ion imbalance and the formation of spherocytes.

Thus, AFM allows not only to accurately determine the basic morphometric parameters of erythrocytes, but also to estimate the ratio of the erythrocyte area/volume, which is one of the important functional characteristics of the cell. A prolonged incubation (60 min) of MNPs with erythrocytes causes a pronounced pathology (characteristic of poikilocytosis and anisocytosis), as well as a change in the charge of erythrocyte membranes and their degradation.

AKNOWLEDGEMENTS

We are sincerely grateful to the staff members of Saratov State University D.A. Gorin and S.V. Herman for the synthesis and provision of magnetite nanoparticles. The work was partially performed on the equipment of the New Materials and Resource-Saving Technologies Center of Collective Use. This work was supported by The Russian Science Foundation, project no. 16-14-10179.

REFERENCES

Asghari-Khiavi, M., Wood, B.R., Mechler, A., Bambery, K.R., Buckingham, D.W., Cooke, B.M., and McNaughton, D., Correlation of atomic force microscopy and raman micro-spectroscopy to study the effects of ex vivo treatment procedures on human red blood cells, *Analyst*, 2010, vol. 135, pp. 525–530.

Borovskaya, M.K., Kuznetsov, E.E., Gorokhova, V.G., Koriakina, L.B., Kurilskaya, T.E., and Pivovarov, Yu.I., Structural and functional characteristics of membrane's erythrocyte and its change at pathologies of various genesis, *Bull. VSNTs SO RAMN*, 2010, vol. 3, no. 73, pp. 334 – 354.

Bulte, J.W. and Kraitchman, D.L., Monitoring cell therapy using iron oxide MR contrast agents, *Curr. Pharm. Biotechnol.*, 2004, vol. 5, pp. 567–584.

Duran, N., Silveira, C.P., Duran, M., Stŭfani, D., and Martinez, T., Silver nanoparticle protein corona and toxicity: a mini-review, *J. Nanobiotechnol.*, 2015, vol. 13, pp. 1–17.

German, S.V., Inozemtseva, O.A., Markin, A.V., Metvally, H., Khomutov, G.B., and Gorin, D.A., Synthesis of magnetite hydrosols in inert atmosphere, *Kolloid. Zh.*, 2013a, vol. 75, no. 4, p. 534.

German, S.V., Inozemtseva, O.A., Navolokin, N.A., Pudovkina, E.E., Zuev, V.V., Volkova, E.K., Bucharskaya, A.B., Pleskova, S.N., Maslyakova, G.N., and Gorin, D.A., Synthesis of magnetite hydrosols and assessment of their impact on living systems at the cellular and tissue levels using MRI and morphological investigation, *Ross. Nanotekhnol.*, 2013b, vol. 8, no. 7–8, pp. 573–580.

German, S.V., Navolokin, N.A., Kuznetsova, N.R., Zuev, V.V., Inozemtseva, O.A., Anis'kov, A.A., Volkova, E.K., Bucharskaya, A.B., Maslyakova, G.N., Fakhrullin, R.F., Terentyuk, G.S., Vodovozova, E.L., and Gorin, D.A., Liposomes loaded with hydrophilic magnetite nanoparticles: preparation and application as contrast agents for magnetic resonance imaging, *Colloids Surfaces B: Biointerfaces*, 2015, vol. 135, pp. 109 – 115.

Grancharov, S.G., Zeng, H., Sun, S., Wang, S.X., O'Brien, S., Murray, C.B., Kirtley, J.R., and Held, G.A., Bio-functionalization of monodisperse magnetic nanoparticles and their use as biomolecular labels in a magnetic tunnel junction based sensor, *J. Phys. Chem. B*, 2005, vol. 109, pp. 13030–13035.

Guo, Q., Liu, Y., Xu, K., Ren, K., and Sun, W.G., Mouse lymphatic endothelial cell targeted probes: anti-LYVE-1 antibody-based magnetic nanoparticles, *Int. J. Nanomed.*, 2013, vol. 9, pp. 2273–2284.

Kozinets, G.I., Shishkanov, Z.G., Sarycheva, T.G., Novotrakhana, Yu.K., Diaghilev, O.A., and Protsenko, D.D., *Kletki krovi i kostnogo mozga. Atlas (Cells of Blood and Bone Marrow: Atlas)*, Moscow: Med. Inform. Agent., 2004.

Leonova, V.G., *Analiz eritrotsitarnykh populyatsy v ontogeneze cheloveka (Analysis of Erythrocyte Populations in Human Ontogeny)*, Novosibirsk: Nauka, 1987.

Nasiri, R., Hamzehalipour, Almaki, J., Idris, A.B., Abdul, Majid, F.A., Nasiri, M., Salouti, M., Irfan, M., Amini, N., and Marvibaigi, M., In vitro evaluation of actively targetable superparamagnetic nanoparticles to the folate receptor positive cancer cells, *Mater. Sci. Eng. C*, 2016, vol. 69, pp. 1147–1158.

Neamtu, J. and Verga, N., Magnetic nanoparticles for magneto-resonance imaging and targeted drug delivery, *Digest J. Nanomat. Biostruct.*, 2011, vol. 6, pp. 969–978.

Novitskii, V.V., Ryazantseva, N.V., Stepovaya, E.A., Bystritskii, L.D., and Tkachenko, S.B., *Atlas. Klinicheskii patomorfoz eritrotsita (Clinical Pathomorphology of Erythrocyte: Atlas), Tomsk: Izd. Dom Tomsk Univ.*, Moscow:: GEOTAR-MED, 2003.

O'Reilly, M., McDonnell, L., and O'Mullane, J., Quantification of red blood cells using atomic force microscopy, *Ultramicroscopy*, 2001, vol. 86, pp. 107–112.

Pankhurst, Q.A., Connolly, J., Jones, S.K., and Dobson, J., Applications of magnetic nanoparticles in biomedicine, *J. Phys. D: Appl. Phys.*, 2003, vol. 36, pp. 167–181.

Pershina, A.G., Sazonov, A.E., and Milto, I.V., Application of magnetic nanoparticles in biomedicine, *Byull. Sib. Med.*, 2008, vol. 2, pp. 70–78.

Pleskova, S.N., *Atomno-silovaya mikroskopiya v biologicheskikh i meditsinskikh issledovaniyakh (Atomic-Force Microscopy in Biology and Medicine), Dolgoprudnyi: Izd.* Dom Intellekt, 2011.

Pleskova, S.N., Pudovkina, E.E., Mikheeva, E.R., and Gorshkova, E.N., Interactions of quantum dots with donor blood erythrocytes in vitro, *Bull. Exp. Biol. Med.*, 2013, vol. 156, no. 3, pp. 384–388.

Skorkina, M.Yu., Fedorova, M.Z., Sladkova, E.A., Derkachev, R.V., and Zabinyakov, N.A., Effect of iron nanoparticles on the respiratory function of blood, *Yaroslav. Ped. Vestn.*, 2010, vol. 3, pp. 75–79.

Yakusheva, E.V., Miroshnikov, S.A., and Kvan, O.V., Estimation of influence of metal nanoparticles on morphological parameters of peripheral blood of animals, *Vestn. Orenburg. Gos. Univ.*, 2013, vol. 12, no. 161, pp. 203–207.

Translated by I. Shipounova